Organic Electronics 10 (2009) 1473–1477

Contents lists available at ScienceDirect

Organic Electronics

journal homepage: www.elsevier.com/locate/orgel

ZnO nano-ridge structure and its application in inverted polymer solar cell

Nobuyuki Sekine [a,b], Cheng-Hsuan Chou [a,c], Wei Lek Kwan [a], Yang Yang [a,*]

[a] Department of Materials Science and Engineering, University of California at Los Angeles, Los Angeles, CA 90095, USA
[b] Fuji Electric Advanced Technology Co. Ltd., Hino-City, Tokyo 191-8502, Japan
[c] Phosphors Research Laboratory, Department of Applied Chemistry, National Chiao Tung University, Hsinchu 30050, Taiwan

ARTICLE INFO

Article history:
Received 11 June 2009
Received in revised form 5 August 2009
Accepted 15 August 2009
Available online 20 August 2009

PACS:
81.07.-b
81.07.Pr
81.20.Fw
84.60.Jt

Keywords:
Polymer solar cell
Inverted polymer solar cell
Zinc oxide
Nano-ridge

ABSTRACT

We report a unique nano-ridge structure of zinc oxide (ZnO) and its application in high performance inverted polymer solar cells. The ZnO nano-ridge structure was formed by a sol–gel process using a ramp annealing method. As the solvent slowly evaporated due to the low heating rate, there was sufficient time for the gel particles to structurally relax and pile up, resulting in a dense and undulated film. Nano-ridges with peak as high as 120 nm and valley to valley distance of about 500 nm were formed. This film provided an effective hole blocking layer and also an increased interfacial area for electron collection. An inverted bulk heterojunction polymer solar cell was fabricated using the ZnO nano-ridge film as the electron collecting layer. The device showed a high power conversion efficiency of 4.00%, an improvement of about 25% over similar solar cells made with a planar film of ZnO nanoparticles.

1. Introduction

There exists significant interest in organic/polymer bulk heterojunction solar cells due to their low temperature and solution processability. Power conversion efficiencies (PCE) have reached over 5–6% through careful control of morphology [1,2] and the use of low band gap materials [3,4]. However, further improvement in efficiency and stability is required. In parallel, highly efficient polymer solar cells using an inverted structure, in which the positions of the anode and cathode are reversed, have been demonstrated [5,6]. The low work function metal, e.g. calcium, used as the cathode in the regular structure, is replaced by a relatively nonreactive electron collection layer. This significantly improves the air stability of the solar cells. Furthermore, vertical phase separation in polymer blends has proven to be advantageous in the inverted structure [7].

One important key to high performance inverted polymer solar cell is the selection of the electron collection layer. The purpose of the electron collection layer is to provide hole blocking capability and a low resistive pathway for efficient electron extraction. $CsCO_3$ [8,9], TiO_2 [10,11], TiO_2:Cs [12] and ZnO [13,14] have been demonstrated to be effective electron collection materials. In particular, ZnO is an attractive material because of the various nanostructures [15,16] that can be easily achieved by solution processing for more efficient charge extraction and transport. For example, Takanezawa et al. [17] has shown that using ZnO nanorods can improve electron transport in bulk heterojunction solar cells. Inspired by these works on ZnO-based inverted solar cells, we designed a simple annealing process to achieve a nano-ridge structure, which has improved hole blocking and electron collection properties. The schematic of the device structure and the scanning electron microscopy (SEM) images of the device and the ZnO nano-ridge structured film are shown in Fig. 1.

* Corresponding author.
E-mail address: yangy@ucla.edu (Y. Yang).

1566-1199/$ - see front matter © 2009 Elsevier B.V. All rights reserved.
doi:10.1016/j.orgel.2009.08.011

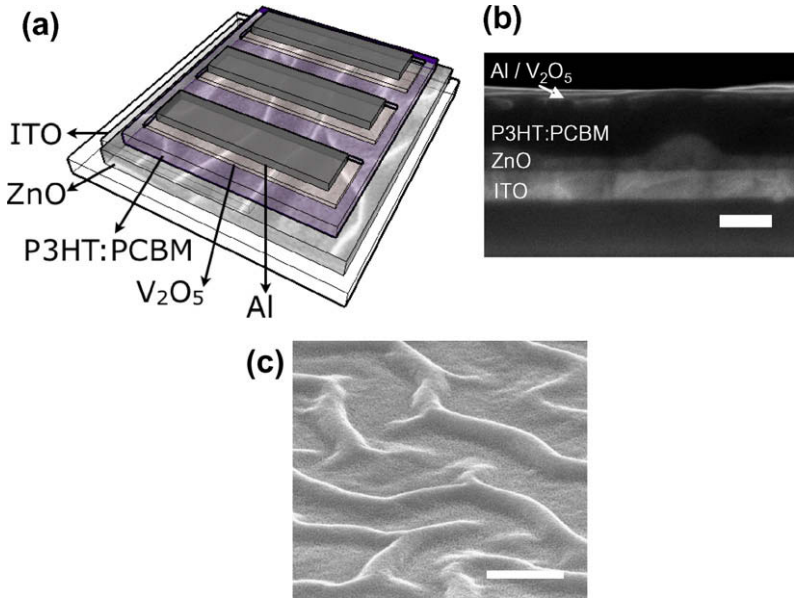

Fig. 1. (a) Device structure, (b) SEM cross-sectional image of the inverted polymer solar cell, scale bar: 200 nm and (c) SEM image of the ZnO nano-ridge film, scale bar: 500 nm.

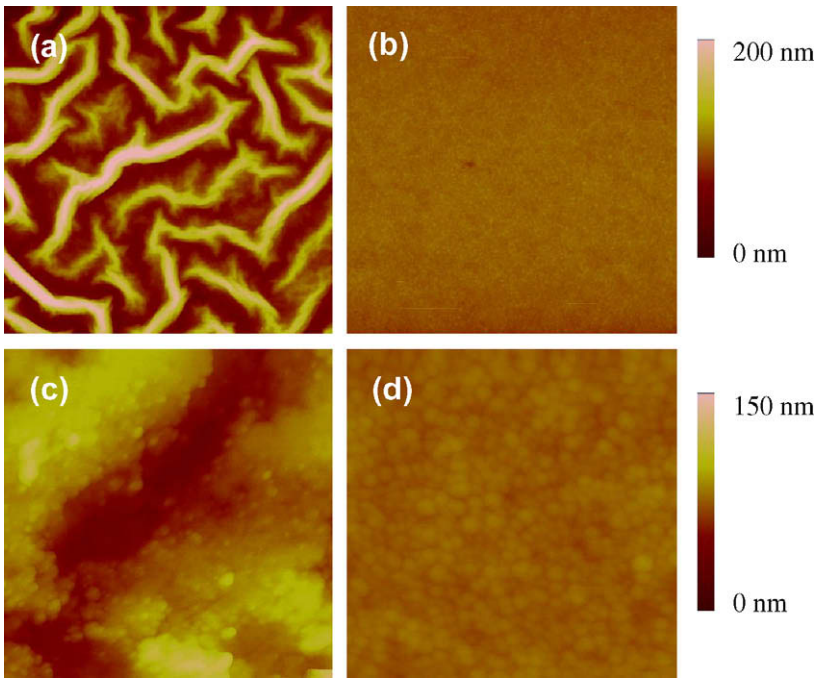

Fig. 2. AFM images of the (a) ZnO nano-ridge and (b) ZnO nanoparticle planar films showing a 5 μm × 5 μm surface area. Close-up AFM images of ZnO nano-ridge (c) and ZnO nanoparticle planar (d) films showing a 500 nm × 500 nm surface area.

2. Experimental

The fabrication of sol–gel processed ZnO nanoparticle films with planar and nano-ridge structures were made from spin coating the same precursor solution but annealing under different conditions. The precursor solution, consisting of 0.75 M zinc acetate dihydrate and 0.75 M monoethanolamine in 2-methoxyethanol [18], was first spun-coated onto indium tin oxide (ITO) substrates at 2000 rpm for 40 s. For the ZnO planar film, the substrate was immediately placed onto a hot plate that was pre-heated at 275 °C and annealed for 5 min. In order to form

the ZnO nano-ridge film, the spin-coated substrate was first placed onto a hot plate that was initially at room temperature while it was still not completely dry. The temperature was then raised at a ramping rate of 50 °C/min to 275 °C and the substrates were subsequently removed from the hot plate when the final temperature was reached. We noticed an increase in sheet resistance of the ITO films when the substrates were heated at higher temperatures, so the annealing temperature the ZnO films was limited at 275 °C. Quartz substrates were used when measuring the transmittance of the ZnO films.

The resulting ZnO films were rinsed in de-ionized water, acetone, and isopropyl alcohol and then dried to remove residual organic material from the surface. All processes thus far were done in ambient air. The substrates were then transferred into a nitrogen-filled glovebox for polymer coating. Poly(3-hexylthiophene) (P3HT) and [6,6]-phenyl C_{61} butyric acid methyl ester (PCBM) blend films were spun-coated onto the substrates from a 1:1 wt-ratio solution in 1,2-dichlorobenzene (20 mg of P3HT/ml of solvent) at 600 rpm using the slow-growth method [1], followed by annealing on a hot plate at 110 °C for 10 min. To complete the solar cell devices, a 10 nm layer of V_2O_5 (serving as a buffer layer for hole collection [8]), following by 70 nm of Al was deposited by thermal evaporation through shadow masks. The device area, as defined by the overlap between the ITO and Al electrodes, was 0.09 cm^2. The solar cells were measured under simulated illumination at AM 1.5 G, 100 mW/cm^2 with a Keithley 2400 source meter controlled by a computer program.

3. Results and discussion

The atomic force microscope (AFM) images of the nano-ridge and planar films are shown in Fig. 2a and b, respectively. Nano-ridges of ZnO nanoparticles with thickness ranging from 50 nm to 120 nm were formed and the valley to valley distance of the nano-ridges was about 500 nm. The ZnO nano-ridge structure was formed by the reorganization of gel particles during the slow drying process [19,20]. The ZnO planar film was relatively smooth with an r.m.s. roughness of about 2.6 nm. The r.m.s. roughness of the nano-ridge film was about 4.0 nm at the top of the ridge. As the morphologies are very different between the two structures, it is difficult to make a direct comparison in the r.m.s. roughness between them. Fig. 2c and d shows the close-up AFM images of the nano-ridge and planar films, respectively.

The transmittance spectra of the ZnO films and absorbance of the ZnO films coated with P3HT:PCBM are shown in Fig. 3. The ZnO nano-ridge film had a slightly lower transmittance over a broad range of wavelengths as compared to the ZnO planar film. This was due to the increase in light scattering by the nano-ridges and was consistent with the white foggy appearance of the film [21]. The polymer films with both types of ZnO morphology showed very similar absorption.

The current–voltage (J–V) characteristics of the solar cell devices with ZnO nano-ridge and planar films under simulated sunlight were shown in Fig. 4a. The device perfor-

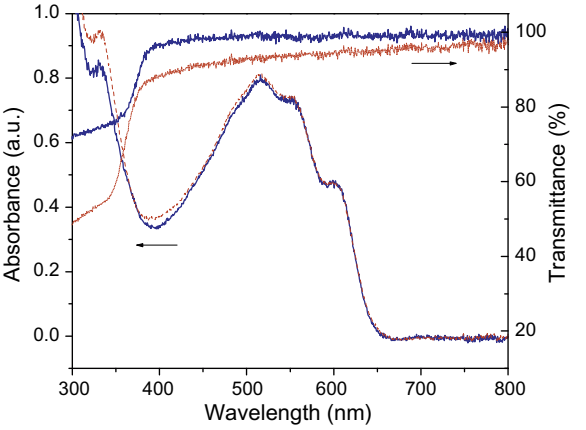

Fig. 3. The absorbance spectra for P3HT:PCBM on ZnO nano-ridge film (dotted line) and planar film of ZnO nanoparticles (bold line) and the transmittance spectra of the nano-ridge film (dotted line) and planar film (bold line).

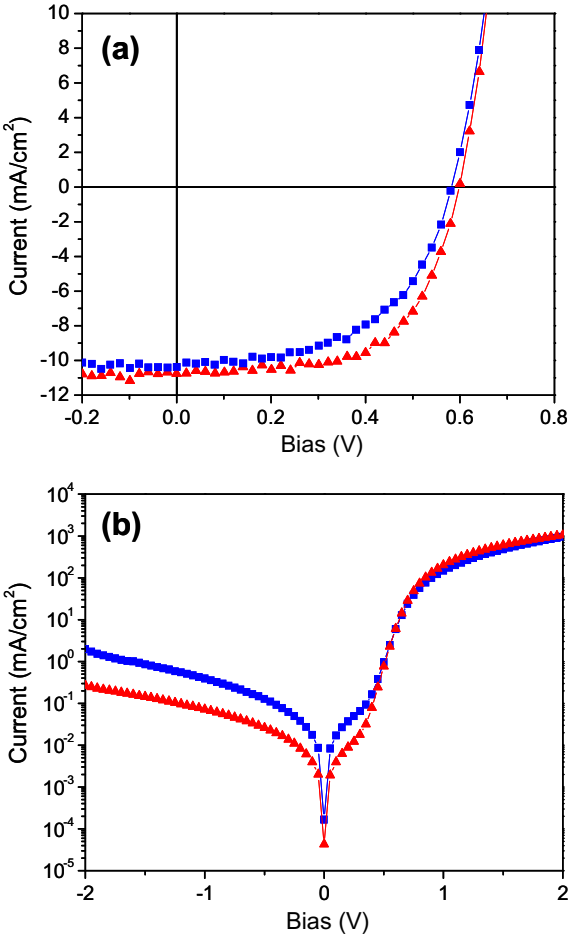

Fig. 4. (a) Current density–voltage (J–V) curves of the ZnO nano-ridge (triangle) and ZnO nanoparticles (square) devices under 100 mW/cm^2 AM 1.5 irradiation. (b) Dark J–V curves of the same devices.

Table 1
The device performance of inverted ZnO polymer solar cells. The values in parentheses are average values over 20 devices.

ZnO structure	Active polymer	V_{oc} (V)	J_{sc} (mA/cm^2)	PCE (%)	FF (%)	R_{shunt}/Ω (cm^2)	R_{series}/Ω (cm^2)
NP	P3HT	0.80 (0.79)	0.19 (0.18)	0.06 (0.05)	44 (42)	4.60E4 (4.26E4)	15.0 (15.3)
NR	P3HT	0.74 (0.74)	0.37 (0.35)	0.15 (0.14)	56 (55)	1.11E5 (1.06E5)	14.3 (14.5)
NP	P3HT:PCBM	0.58 (0.58)	10.41 (10.35)	3.20 (3.06)	53 (51)	2.30E4 (1.77E4)	1.4 (1.6)
NR	P3HT:PCBM	0.60 (0.60)	10.76 (10.57)	4.00 (3.87)	62 (61)	1.42E5 (1.11E5)	1.4 (1.5)

mance is summarized in Table 1. The ZnO nano-ridge device showed a remarkable improvement over the device with the planar film. The average power conversion efficiency of 20 devices fabricated with nano-ridge films was 3.87%, while devices with planar films showed an efficiency of only 3.06%. The best device performance obtained from the nano-ridge device was 4.00%. The major improvement in device performance arises from the higher fill factor (FF) of the ZnO nano-ridge device, while the open circuit voltage (Voc) and short-circuit current density (Jsc) remained almost unchanged. This is reflected in the series and shunt resistance as well. The shunt resistance showed a difference of about an order of magnitude while the series resistance was almost the same. Thus, it is unlikely that the improvement in the device performance is due to the change in carrier concentration or work function. We attributed this enhancement to lower leakage current due to the improvement in hole blocking capability and electron collection efficiency of the nano-ridge structured film.

The dark *J–V* curve (Fig. 4b) shows a lower leakage and higher forward bias current for the ZnO nano-ridge device, indicating better charge selectivity over the ZnO planar film. This is due to the difference in the packing density of the films. As the ZnO nano-ridge film is formed by a slower heating process, there is sufficient time for the gel film to structurally relax before crystallizing, resulting in a denser film [18] than that of ZnO planar film [22]. A denser film with fewer defects would be more effective in blocking the transport of holes, leading to lower leakage current, i.e. a larger shunt resistance and higher FF.

To clarify whether the nano-ridge structure of the ZnO played a role in improving charge extraction, bilayer devices without PCBM were also fabricated. The Jsc for the ZnO nano-ridge bilayer device was close to two times higher than that of the device with the ZnO planar film, indicating a much larger interfacial area for charge separation. Similar to the results of ZnO nanorods [22,23], we believe that our ZnO played a comparable role, albeit a smaller one, to that of the ZnO nanorods-based solar cells. The larger surface area of electrode contact and undulate network structure minimized the distance charge carriers need to travel in the active polymer to reach the electrodes.

4. Conclusion

We reported a ZnO nano-ridge structured film that can be formed by a simple ramp annealing process. The nano-ridge structure has comparable excellent electron collection properties as that of ZnO nanorods and yet can be made with similar simple fabrication processes as the ZnO planar film. The effect of the viscosity of the solution and the solvent evaporation rate on the nano-structured pattern is to be further studied. Both inverted bulk heterojunction polymer solar cells and ZnO:P3HT hybrid solar cells showed remarkable improvements in efficiency when the ZnO nano-ridge structure was used. We attributed the improvement in FF to higher electron selectivity and more efficient charge collection, leading to a 4.00% inverted polymer solar cell.

Acknowledgments

The authors would like to thank Dr. Ziruo Hong, Mr. Raymond Chen and Mr. Bao Lei from UCLA for technical discussion, and financial support from Office of Naval Research (Fund No. N00014-04-1-0434). In addition, N. Sekine would also like to thank Fuji Electric Advanced Technology Co., Ltd. for granting him a sabbatical leave for conducting this research. C.H. Chou would also like to thank the National Science Council of Taiwan, Project NSC-0962917-I-009-112 for financial support.

References

[1] G. Li, V. Shrotriya, J. Huang, Y. Yao, T. Moriarty, K. Emery, Y. Yang, Nat. Mater. 4 (2005) 864.
[2] M.L. Ma, C.Y. Yang, X. Gong, K. Lee, A.J. Heeger, Adv. Funct. Mater. 15 (2005) 1617.
[3] J. Peet, J.Y. Kim, N.E. Coates, W.L. Ma, D. Moses, A.J. Heeger, G.C. Bazan, Nat. Mater. 6 (2007) 497.
[4] J. Hou, H.Y. Chen, S. Zhang, G. Li, Y. Yang, J. Am. Chem. Soc. 130 (2008) 16144.
[5] S.K. Hau, H.L. Yip, N.S. Baek, J. Zou, K. O'Malley, A.K.Y. Jen, Appl. Phys. Lett. 92 (2008) 253301.
[6] L.M. Chen, Z. Hong, G. Li, Yang Yang, Adv. Mater. 21 (2009) (published online).
[7] Z. Xu, L.M. Chen, G.W. Yang, C.H. Huang, J. Hou, Y. Wu, G. Li, C.S. Hsu, Y. Yang, Adv. Funct. Mater. 19 (2009) (published online).
[8] G. Li, C.W. Chu, V. Shrotriya, J. Huang, Y. Yang, Appl. Phys. Lett. 88 (2006) 253503.
[9] H.H. Liao, L.M. Chen, Z. Xu, G. Li, Y. Yang, Appl. Phys. Lett. 92 (2008) 173303.
[10] C. Waldauf, M. Morana, P. Denk, P. Schilinsky, K. Coakley, S.A. Choulis, C.J. Brabec, Appl. Phys. Lett. 89 (2006) 233517.
[11] G.K. Mor, K. Shankar, M. Paulose, O.K. Varghese, C.A. Grimes, Appl. Phys. Lett. 91 (2007) 152111.
[12] Mi-Hyae Park, Juo-Hao Li, Ankit Kumar, Gang Li, Yang Yang, Adv. Mater. 19 (2009) 1241.
[13] M.S. White, D.C. Olson, S.E. Shaheen, N. Kopidakis, D.S. Ginley, Appl. Phys. Lett. 89 (2006) 143517.

[14] A.K.K. Kyaw, X.W. Sun, C.Y. Jiang, G.Q. Lo, D.W. Zhao, D.L. Kwong, Appl. Phys. Lett. 93 (2008) 221107.
[15] L. Vayssieres, Adv. Mater. 15 (2003) 464.
[16] Z. Wang, X.F. Qian, J. Yin, Z.K. Zhu, Langmuir 20 (2004) 3441.
[17] K. Takanezawa, K. Tajima, K. Hashimoto, Appl. Phys. Lett. 93 (2008) 063308.
[18] M. Ohyama, H. Kozuka, T. Yoko, Thin Solid Films 306 (1997) 78.
[19] R.D. Deegan, O. Bakajin, T.F. Dupont, G. Huber, S.R. Nagel, T.A. Witten, Nature 389 (1997) 827.
[20] E. Rabani1, D.R. Reichman, P.L. Geissler, L.E. Brus, Nature 426 (2003) 271.
[21] Y.S. Kim, W.P. Tai, S.J. Shu, Thin Solid Films 491 (2005) 153.
[22] K. Takanezawa, K. Hirota, Q.S. Wei, K. Tajima, K. Hashimoto, J. Phys. Chem. C 111 (2007) 7218.
[23] D.C. Olson, S.E. Shaheen, R.T. Collins, D.S. Ginley, J. Phys. Chem. C 111 (2007) 16670.